ELSEVIER

Applied Surface Science 175–176 (2001) 129–133

applied surface science

www.elsevier.nl/locate/apsusc

# Electromigration of single-layer clusters

O. Pierre-Louis[a,*], T.L. Einstein[b]

[a]*LPS Grephe, UJF (CNRS), Grenoble I, BP 87, 38402 St. Martin d'Heres, France*
[b]*Department of Physics, University of Maryland, College Park, MD 20742-4111, USA*

Accepted 30 January 2001

**Abstract**

We describe the steady states, fluctuations, dynamics, and instabilities of atom and of vacancy single-layer-height islands during electromigration, assuming an isotropic medium. We emphasize the dependence on cluster size and on the three standard limiting cases of mass-transport mechanism: periphery diffusion (PD), terrace diffusion (TD), or evaporation–condensation (EC), as well as the differences between atom and vacancy clusters. A general model provides power laws describing the size dependence of the drift velocity in these limits, consistent with established (in the case of PD) results. For PD, atom and vacancy islands drift in opposite directions; otherwise they drift in the same direction. The validity of the widely used quasistatic limit is calculated. Linear stability analysis reveals a new type of morphological instability, not leading to island break-down. We find non-circular steady states for EC vacancy islands. Analytical calculations are corroborated by both Monte Carlo simulations and numerical integration. For weak electromigration the cluster responds isotropically for TD and PD but not EC. In EC, clusters elongate perpendicular to the drift axis. In PD a morphological instability at strong electromigration leads to cluster splitting, in contrast to destabilizing into slits in the other cases. TD or EC induces a new instability for vacancy clusters above a threshold. Using Langevin formalism, we derive the non-equilibrium cluster diffusion constant and study morphological fluctuations. Electromigration affects the diffusion coefficient of the cluster and morphological fluctuations, which diverge at the instability threshold. An instrinsic attachment–detachment bias displays the same scaling signature as PD in the drift velocity. © 2001 Published by Elsevier Science B.V.

*PACS:* 66.30Aa; 05.70.Ln; 68.35.Fx; 36.40.Sx

*Keywords:* Electromigration; Single-layer clusters; Periphery diffusion

## 1. Introduction

This paper presents a summary of a paper that has appeared in print [1] since ICSFS-10. It capsulizes the important results and presents a new figure. Our research on this subject has the following motivations: First, electromigration is a technologically important subject that also presents problems that are becoming tractable for condensed matter physicists. There has been noteworthy progress in the theory of bulk electromigration, and generalizations to surface problems are possible. Second, the subject provides another venue in which we test the continuum step model, which posits that a wide range of mesoscopic and macroscopic phenomena can be described in terms of the step stiffness, the interaction strength of the repulsion between steps, and a coefficient characterizing mass transport, such as a kinetic coefficient or the product of mass carriers and their associated diffusion

* Corresponding author.

0169-4332/01/$ – see front matter © 2001 Published by Elsevier Science B.V.
PII: S0169-4332(01)00160-X

Table 1
Table of important parameters[a]

| | |
|---|---|
| $\xi \equiv k_B T/F$ | Characteristic length associated with electromigration |
| $D$ | Diffusion constant for adatoms on terraces |
| $D_{st}$ | Diffusion constant for motion of edge-atom atoms along the step |
| $D_c$ | Diffusion constant for clusters |
| $v_\pm$ | Kinetic coefficients for attachment/detachment at lower/upper step-edge side |
| $d_\pm \equiv D/v_\pm$ | Corresponding attachment length, $\propto$ attachment/detachment rate |
| $a$ | Lattice constant |
| $\Gamma = a^2\overline{\beta}/k_B T$ | Capillary length |
| $c_{eq}^0$ | Equilibrium concentration near a straight step |
| $c_{st}$ | Concentration of mobile edge-atoms |
| $\kappa$ | Step curvature (positive for a convex step) |
| $\tilde{\beta}(\theta)$ | Step stiffness, assumed isotropic ($\tilde{\beta}(\theta) = \tilde{\beta}$) |
| $D_L \equiv a^2 c_{st} D_{st}$ | Macroscopic step diffusion constant |
| $W^2 \equiv \langle R^2\rangle - \langle R\rangle^2$ | Island roughness |

[a] In typical experimental conditions, $\xi \sim 10^8 a$ for Si and $\xi \sim 10^5 a$ for metals. When $d_\pm$ are small, the dynamics are diffusion limited (TD). The Gibbs–Thomson relation indicates that at the step edge, $c_{eq} = c_{eq}^0 \exp(\Gamma\kappa)$.

constant — without calculating or specifying microscopic energy barriers for mass motion. Third, various controversies have arisen regarding the dominant mode of mass transport (attachment/detachment limited (AD, alternatively called EC, i.e. evaporation/condensation), terrace diffusion (TD), or periphery diffusion (PD)) for specific systems when comparing data for step fluctuations and for the diffusion of (undriven) atom or vacancy clusters. Electromigration of such clusters evidently provides several new phenomena that can be used to distinguish these three types of behavior. Fourth, electromigration, being a driven system, develops various instabilities. While to date we have focussed on the linear regime, there are tantalyzing non-linear effects to be explored.

A major result for the thermal diffusion of nearly circular single-layer clusters of adatoms or vacancies, discussed extensively by Khare et al. [2–5], is that the tracer diffusion constant $D_c^{eq}$ has distinctive size dependence,

$$D_c^{eq} \sim R_0^{-\alpha} \tag{1}$$

with $\alpha = 3,\ 2$, and 1 for PD, TD, and EC, respectively. Here $R_0$ is the (average) radius of the cluster. In the present investigations, we add an electromigration force $F$, taking it to be along the $x$-axis. $R$ is the distance from the center of the island, $\theta$ the polar angle with respect to the $x$ axis, and $s$ the arclength along the step. $R_0$ is the mean radius. Other parameters needed are listed and defined in Table 1. For the drift speed of the cluster, we now find

$$|\overline{V}| \approx D_c^{eq} \frac{\pi R_0^2 F}{a^2 k_B T} \sim R_0^{2-\alpha} \tag{2}$$

Thus, by looking at the electromigration of a set of clusters and examining whether the drift speed decreases, stays the same, or increases with increasing radius, we get an independent indication of whether PD, TD, or EC dominates. We now consider each of these cases individually and describe salient findings.

## 2. Periphery-diffusion (PD) limit

When dynamics are dominated by motion along the cluster boundary, we saw in Eq. (2) that the drift speed varies inversely with radius. More specifically we find the drift velocity to be

$$V = \phi \frac{a D_L}{\xi_{st} R_0} \tag{3}$$

where $\phi = 1\,(-1)$ denotes atom (vacancy) islands. Thus, in this case atom islands and vacancy clusters drift in *opposite* directions. For plausible values of the parameters for metals At 600 K on metals $\xi_{st} \approx 10^5$ Å. For a concentration of mobile atoms per site $c_{st} \approx 0.1$, $D_L \approx 10^9$ Å$^2$/s; for $R_0 \approx 10^3$ Å, the order of magnitude of the drift speed is 10Å/s [1].

Next, we define a dimensionless force

$$\chi \equiv \frac{R_0^2}{\Gamma\xi} = \left(\frac{F}{\tilde{\beta}}\right)\left(\frac{R_0}{a}\right)^2 \tag{4}$$

For $|\chi|$ sufficiently large, the cluster becomes unstable. Linear stability analysis shows that the critical value for instability is $\chi_c = 10.65$. With the preceding parameters and $\tilde{\beta} = 0.3\,\mathrm{eV}/a$, islands with $R_0 > R_c \approx 5 \times 10^3$ Å are unstable. The characteristic time for instabilities to appear, $\tau = \chi_c \Gamma\xi/(aD_L)$ is of order $10^2$ s; hence, this instability should be experimentally observable.

Since observables such as $D_c$ and the roughness should not depend on the direction of the force, we expect non-linear corrections to include only even powers of $\chi$. To leading order we find

$$D_c = D_c^{eq}(1 + \tfrac{1}{4}\chi^2 + O(\chi^4)),$$
$$W^2 = W_{eq}^2(1 + 0.23\chi^2 + O(\chi^4)) \tag{5}$$

The equilibrium values are $D_c^{eq} = a^3 D_L/\pi R_0^3$ and $W_{eq}^2 = 3k_B T R_0/4\tilde{\beta}$. Furthermore, $W \sim (\chi_c - \chi)^{-1/2}$.

To corroborate our analysis, we performed kinetic Monte Carlo simulations for a vacancy island (so in the PD limit analogous to a conducting void). We choose $F = 0.1\varepsilon/a$ and $k_B T = 0.6\varepsilon$, where the characteristic energy $\varepsilon$ is the energy of a single bond in our simple model. The instability appears for radii larger than $\approx 13a$. The results are depicted in Fig. 3 of [1]. For a radius of $10a$ the island is stable. For long times, it develops a slight elongation, probably due to unavoidable anisotropies. When the radius is $15a$, the island is unstable to splitting. The same instability occurs for atom islands.

## 3. 2D transport regime: TD and EC

When transport is dominated by carriers leaving from and arriving at the cluster, i.e. when strict mass conservation does not hold, then the equilibrium diffusion constant takes the form

$$D_c^{eq} = \frac{a^4 D c_{eq}^0}{\pi R_0}\left(\frac{1}{R_0 + d_+} + \frac{1}{R_0 + d_-}\right) \tag{6}$$

To first order in $\xi^{-1}$, the islands stay circular and drift with

$$\overline{V} = -\frac{a^2 D c_{eq}^0}{\xi}\left(\frac{R_0}{R_0 + d_+} - \frac{R_0}{R_0 + d_-}\right) \tag{7}$$

There are several important consequences of these key results

- In order to have non-zero drift, $d_-$ and $d_+$ must differ. This is the case for a normal Ehrlich–Schwoebel effect, corresponding to $d_- > d_+$.
- For EC, occurring when both $d_\pm \gg R_0$, $\overline{V}$ *increases* with the size of the cluster.
- Eq. (7) reproduces the result that Wickham and Sethna [6] obtained using Monte Carlo simulations: $|\overline{V}| = v_0 - v_1(a/R_0)$ for $R_0 \gg d_+$ (and $d_- \to \infty$), so that $v_0 = a^2 D c_{eq}^0/\xi$ and $v_1 = v_0 d_+/a$.
- Both atom and vacancy islands drift in the *same* direction, opposite to the electromigration force (for $d_- > d_+$, typical Ehrlich–Schwoebel).

For a vacancy or an atom cluster in the TD limit, the circular steady state is an exact solution of the equations of motion (even in the non-quasistatic limit) for instantaneous attachment ($d_+ = 0$). For finite $d_+$ the steady state of the interior model (viz. a vacancy island with an infinite Ehrlich–Schwoebel barrier) has a non-circular shape, at least to second order in $\xi^{-1}$. This shape is elongated perpendicular to the electromigration force for vacancy islands (along the electromigration force for atom islands), this phenomenon is analogous to the Bernoulli effect, as illustrated in Fig. 1. Quantitatively, the fractional elongation (the difference of the vertical and horizontal "diameters" divided by the mean diameter) is

$$\Delta = \frac{1}{\Gamma}\frac{R_0^1}{6\xi^2}\frac{d_+ R_0}{d_+ + R_0} \tag{8}$$

In the EC limit, with $R_0 \sim 10^3 a$ and $\xi \sim 10^5 a$, one finds that $\Delta \sim 10^{-2}$: the deformation is small. When mass exchange with the exterior is allowed, as for an atom island, there is no steady state.

Further analysis shows that the commonly used quasistatic limit is valid when $\Gamma a^2 \tilde{c}_{eq} v_+ \ll D$, i.e. when the effective diffusion constant of the step (l.h.s.) is much smaller than that of adatoms on the terrace (r.h.s.). This inequality is valid in the limit of slow kinetics (EC: $v_+ \ll D/a$); for fast-kinetics (TD), it holds when $a\Gamma\tilde{c}_{eq} \ll 1$. For example, Si(1 1 1) at $T \sim 1000$ K is a case of slow kinetics: $a^2 c_{eq} < 0.1$, $d_+ = D/v_+ \sim 10^4 a$, and $\Gamma \sim 10$ Å. Thus, the quasistatic approximation is satisfactory.

As in the PD case, we corroborate our analysis using kinetic Monte Carlo simulations for a vacancy

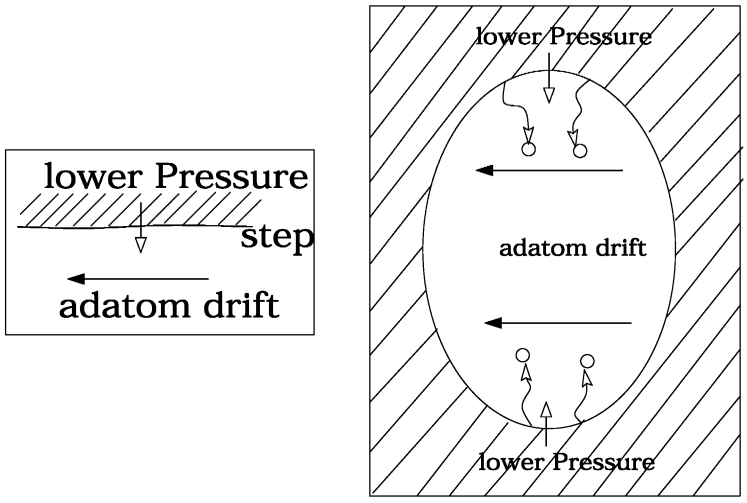


Fig. 1. Illustration of the Bernoulli-like effect causing elongation (quadruple deformation) of a vacancy island perpendicular to the drift direction $\hat{x}$. Viewed alternatively, atoms detaching from the sides not only drift along $\hat{x}$ but also have a residual drift toward the center if they have a small sticking probability. For an atom island, the motion is outside rather than inside the island, producing the opposite sign for the deformation: elongation along $\hat{x}$.

cluster, but with adatoms now allowed inside. At high temperature $k_BT \geq 0.7\varepsilon$, micro-vacancies escape noticeably from the steps. Hence, we select $k_BT = 0.6\varepsilon$ as before, with the same value of $F$. No drastic change in the island shape is seen at the linear-stability threshold. Let us define the front and the back side of the island with respect to cluster motion as the first and the last part passing at a given value of $x$. For increased electromigration, the front, leading side of the cluster is stabilized. The back, trailing side is destabilized and exhibits chaotic behavior, but its roughness remains finite. For stronger electromigration force, unstable slit-like shapes appear. Since these shapes are seen for all orientations of **F**, they are not due to lattice anisotropy. Fig. 4 of [1] provides illustrations. This instability contrasts qualitatively with the splitting found in the PD regime.

## 4. Summary and perspectives

A summary of our results is presented in Table 2, adapted slightly from [1]. We emphasize that

Table 2
Tabulation of results[a]

| | PD | TD | EC (AD) |
|---|---|---|---|
| Length criterion | $R_0^2 \ll (R_0+d)D_L/aDc_{eq}^0$ | $R_0 \gg d_+$ or $d_-$ | $R_0 \ll d_+$ and $d_-$ |
| $\langle V(R_0)\rangle$ | $1/R_0$ | 1 | $R_0$ |
| Atom/vacancy drift direction | Opposite | Same | |
| Steady state shape | Circular | | None<br>Non-circular |
| Instability morphology | Splitting | ''Slit'' $\parallel$ **F**<br>Slit $\perp$ **F** | |
| $D_c$ | $D_c^{eq}(1+\frac{1}{4}\chi^2)$ | Anisotropic | |

[a] In general the entries apply to both atom and vacancy islands. The criteria for the three regimes in terms of the characteristic lengths are given in the first row. The inequality for PD is dominant; when it holds, one has PD even if the inequality for TD or EC is satisfied. In the fourth and fifth rows, the upper (lower) entry is for atom/exterior (vacancy/interior) islands.

electromigration provides readily observable ways by which one can distinguish the three modes of mass transport. For PD the drift velocity and shape changes agree with earlier results [7]. Fluctuations are found to be affected by electromigration. The island roughness diverges as the instability threshold is approached.

Especially at low temperature, anisotropy should be included [6,8–10] for a more realistic description. Experiments already show that extremely anisotropic properties (such as diffusion) can alter behavior significantly [11]. Finally, a fuller understanding of the instabilities requires a non-linear analysis.

## Acknowledgements

This work supported by the NSF-sponsored MRSEC at University of Maryland.

## References

[1] O. Pierre-Louis, T.L. Einstein, Phys. Rev. B 62 (2000) 13697.
[2] S.V. Khare, N.C. Bartelt, T.L. Einstein, Phys. Rev. Lett. 75 (1995) 2148.
[3] S.V. Khare, T.L. Einstein, Phys. Rev. B 54 (1996) 11752.
[4] S.V. Khare, T.L. Einstein, Phys. Rev. B 57 (1998) 4782.
[5] S.V. Khare, T.L. Einstein, in: P.M. Duxbury, T. Pence (Eds.), Dynamics of Crystal Surfaces and Interfaces, Plenum Press, New York, 1997, p. 83.
[6] L.K. Wickham, J.P. Sethna, Phys. Rev. B 51 (1995) 15017.
[7] P.S. Ho, J. Appl. Phys. 41 (1970) 64.
[8] M. Schimschak, J. Krug, Phys. Rev. Lett. 80 (1998) 1674.
[9] M. Schimschak, J. Krug, J. Appl. Phys. 87 (2000) 695.
[10] M.R. Gungor, D. Maroudas, Appl. Phys. Lett. 72 (1998) 3452.
[11] J.J. Métois, J.-C. Heyraud, A. Pimpinelli, Surf. Sci. 420 (1999) 250.